Published Online: 2026 January 21 **Research Article**

Preparation and Characterization of HP-β-Cyclodextrin-Integrated Chitosan Nanoparticles for Non-invasive Insulin Delivery

Ali Rajabiyan [1], Mosadegh Keshavarz [2], Amanollah Zarei-Ahmady [1,*], Ghazaleh Shakiba Maram [3]

[1] Marine Pharmaceutical Science Research Center, Ahvaz Jundishapur University of Medical Sciences, Ahvaz, Iran
[2] Department of Chemistry, Yasouj University, Yasouj, Iran, P.O. Box 353, 75918-74831
[3] Student Research Committee, Ahvaz Jundishapur University of Medical Sciences, Ahvaz, Iran

[*] ***Corresponding Author:*** Department of Medicinal Chemistry, Faculty of Pharmacy, Ahvaz Jundishapur University of Medical Sciences, Ahvaz, Iran. Email: zarei-a@ajums.ac.ir

Received: 1 November, 2025; **Revised:** 24 December, 2025; **Accepted:** 27 December, 2025

Abstract

Background: Diabetes affects over 537 million adults globally, with insulin therapy remaining essential — particularly for type 1 diabetes. However, the oral delivery of insulin is hindered by poor bioavailability due to enzymatic degradation, low permeability, and mucosal barriers.

Objectives: The main goal of this project was to design and evaluate a nanocarrier made of chitosan (CS) incorporated with 2-hydroxypropyl-β-cyclodextrin (HP-β-CD) for the delivery of insulin.

Methods: The composite was prepared by the ionic gelation of CS with sodium tripolyphosphate (TPP) as a crosslinker.

Results: The optimized nanocarrier (0.2% CS, 1.5 mg/mL TPP, six mM HP-β-CD) exhibited a particle size of 62.5 nm. The insulin complexation with HP-β-CD facilitates insulin entrapment over the nanoparticle (NP) surface. The inclusion complex was analyzed in solution through phase solubility diagrams. The stability constant was calculated at different temperatures (10, 25, and 37°C; pH = 4.6) to determine the thermodynamic parameters of inclusion. The release profile showed insulin was released rapidly (70% insulin in 20 min).

Conclusions: The engineered TPP/HP-β-CD/CS nanocarrier demonstrates high efficiency in encapsulating insulin, enhances its solubility and stability, and enables rapid release, making it a promising candidate for oral or nasal delivery of macromolecular drugs.

Keywords: Drug Delivery, Nanocomposite, Natural Polymer, Ionic Gelation, In-vitro Release, Hydroxypropyl-β-Cyclodextrin

1. Background

According to a 2021 report by the International Diabetes Federation, approximately 537 million adults worldwide (aged 20 - 79) are living with diabetes, and this number is projected to rise to 643 million by 2030 (1). The two main types of diabetes are classified based on their underlying pathophysiological mechanisms. Insulin therapy remains the only effective treatment for type 1 diabetes and is essential for blood glucose regulation (2, 3). Human insulin is a polypeptide with a molecular mass of around 6000, consisting of two peptide chains that contain a total of 51 amino acids (4, 5).

The parenteral administration of macromolecular drugs can cause pain, stress associated with repeated injections, and potential infections. Although alternative routes such as oral or nasal delivery offer greater convenience and improved patient compliance, most macromolecular drugs exhibit poor bioavailability via these routes (6, 7). This low bioavailability is primarily attributed to poor aqueous solubility and limited permeability across biological membranes (8). Due to various physiological barriers — including enzymatic degradation, poor intestinal absorption, and

How to Cite: Rajabiyan A, Keshavarz M, Zarei-Ahmady A, Shakiba Maram G. Preparation and Characterization of HP-β-Cyclodextrin-Integrated Chitosan Nanoparticles for Non-invasive Insulin Delivery. Jundishapur J Nat Pharm Prod. 2026;21(1):e167615. doi: https://doi.org/10.5812/jjnpp-167615

mucociliary clearance — the use of nanocarriers capable of traversing mucosal surfaces and delivering therapeutic molecules represents a promising strategy to overcome these challenges (9-11).

Chitosan (CS), a deacetylated derivative of chitin, has been widely used — particularly in nanostructured form — for drug delivery applications (12, 13). This naturally abundant polymer is biodegradable and biocompatible (14), and it is soluble in organic acids but generally insoluble in inorganic acids such as phosphoric and sulfuric acid (15). Many researchers have used micro- and nanoparticles (NPs) of CS in mucosal drug delivery due to its mucoadhesive properties and mild encapsulation conditions (14, 16).

Cyclodextrins (CDs) are cyclic oligosaccharides composed of glucose units linked by α-1,4-glycosidic bonds and are produced from starch via enzymatic conversion. These compounds find applications in diverse fields, including pharmaceuticals, drug delivery, food processing, chemical industries, agriculture, and environmental engineering. They enhance the bioavailability of non-polar drugs by improving their aqueous solubility through the formation of inclusion complexes (17). Moreover, the physicochemical properties of drugs are altered upon incorporation into the hydrophobic cavity of CDs (18, 19). The CD complexation represents an effective strategy for improving macromolecular drug therapy by stabilizing the drug against aggregation and enzymatic degradation (20). Furthermore, CDs function as enhancers of solubility and permeability for incorporated macromolecular drugs (21) and can also inhibit the activity of specific proteases (22).

β-Cyclodextrin (β-CD) reduces insulin adsorption onto hydrophobic surfaces and minimizes self-aggregation at neutral pH due to its hydrophilic nature (23). Insulin delivery systems utilizing β-CD or carboxymethyl-β-CD grafted onto CS NPs have been previously reported (24-26). 2-Hydroxypropyl-β-cyclodextrin (HP-β-CD) exhibits greater water solubility than β-CD and carboxymethyl-β-CD, and its reduced renal toxicity facilitates parenteral administration (27, 28). Consequently, HP-β-CD has been successfully employed in the delivery of metronidazole and various anticancer agents (29, 30). Notably, Sajeesh and Sharma demonstrated a similar approach for oral insulin delivery using HP-β-CD (31). The mucoadhesive properties of CS combined with the molecular size selectivity and transport-enhancing capabilities of HP-β-CD may synergistically yield a superior drug carrier (32, 33).

2. Objectives

This study introduces a novel nanocarrier system by synergistically integrating HP-β-CD into CS NPs via ionic gelation with tripolyphosphate (TPP), specifically engineered for efficient oral or nasal delivery of insulin — a notoriously challenging macromolecular drug. Unlike conventional CS-based carriers, the incorporation of HP-β-CD not only enhances insulin solubility and stability through host–guest complexation but also mitigates aggregation and improves encapsulation efficiency. The optimized TPP/HP-β-CD/CS nanohybrid demonstrates rapid insulin release (70% within 20 min), a feature particularly advantageous for mucosal absorption, while simultaneously protecting insulin from enzymatic degradation and low-permeability barriers. This dual-function design — combining the mucoadhesive properties of CS with the solubilizing and stabilizing capabilities of HP-β-CD — represents a significant advancement over existing nanocarriers, offering a promising non-invasive alternative to parenteral insulin therapy. Herein, we introduce an insulin nanocarrier that demonstrates the benefits of CS NPs by increasing drug permeance through epithelia and the solubilizing power of CD regarding its ability to increase drug bioavailability.

3. Methods

3.1. Materials

The HP-β-CD (average degree of substitution: 0.6 mol of 2-hydroxypropyl per glucose unit), CS (Mw ~21 kDa, 93% deacetylated), and sodium TPP were purchased from Sigma-Aldrich. Insulin was obtained from Novo Nordisk (Bagsværd, Denmark). Scanning electron microscopy (SEM) was used to determine the size and morphology of the NPs using a Hitachi S-4160. Fourier-transform infrared (FT-IR) spectra were recorded with an FT-IR-8400S spectrophotometer (Shimadzu, Japan, KBr disk).

3.2. Synthesis of Chitosan/2-Hydroxypropyl-β-Cyclodextrin/Sodium Tripolyphosphate Nanoparticles

The ionotropic gelation method was employed for the synthesis of NPs (34). Aqueous solutions of HP-β-CD (1.5 mL, 4 - 8 mM) were magnetically stirred with 1.5 mL of CS solution (0.1 - 0.4% w/v) for 24 h and subsequently filtered through cellulose acetate membranes (pore size: 0.45 µm). Under continuous magnetic stirring, 1 mL of sodium TPP solution (1 - 2 mg/mL), serving as a crosslinking agent, was added dropwise to the filtrate, thereby inducing crosslinking of CS and facilitating NP formation. The resulting NPs were collected by centrifugation at 13,500 rpm for 30 min. The production yield was determined by weighing the dried NPs and expressing the value as a percentage of the total initial mass of CS and TPP (Table 1). The optimized formulation was characterized using UV-Vis and FT-IR spectroscopy, and SEM.

3.3. Preparation of Insulin/Chitosan/2-Hydroxypropyl-β-Cyclodextrin/Sodium Tripolyphosphate Nanoparticles

Insulin-loaded CS/HP-β-CD/sodium TPP nanocomplexes were formed via electrostatic interactions. Insulin was loaded by adding it to the pre-formed CS/HP-β-CD solution, followed by stirring for 24 h. The resulting suspension was analyzed spectrophotometrically to determine the insulin content. After 24 h, 0.75 mL of TPP solution (2 mg/mL) was added to the CS/HP-β-CD/insulin mixture, and the final suspension was stirred for an additional hour. The drug-loaded NPs were then isolated by centrifugation at 13,500 rpm for 30 min.

3.4. Phase Solubility Studies

The phase solubility method described by Higuchi and Connors was employed to investigate the formation of inclusion complexes between insulin and the nanocarrier (35). Briefly, 10 mL of acetate buffer (pH = 4.6) containing HP-β-CD at concentrations ranging from 4 to 8 mM was placed in sealed glass vials. A 0.5 mL aliquot of insulin solution (14.2 mg/mL) was added to each vial, along with CS (0.2% w/v). The mixtures were stirred at 10, 25, and 37°C until equilibrium was reached (72 h). The samples were then filtered through 0.45 µm cellulose acetate membranes, and the insulin concentration in the filtrate was determined spectrophotometrically at 274 nm against a pre-established calibration curve. The apparent 1:1 stability constants (K1:1) were calculated from the slope of the linear portion of the phase solubility diagrams using (35):

$$K_{1:1} = Slope/S_0\ (1 - Slope)$$

where S_0 is the intrinsic solubility of insulin in the absence of HP-β-CD (i.e., the y-axis intercept). Thermodynamic parameters — including the standard Gibbs free energy change (ΔG), enthalpy change (ΔH), and entropy change (ΔS) — were derived from the temperature dependence of the stability constants (36). The relationship between ΔG and the equilibrium constant is given by:

$$\Delta G = -RT\ lnK1:1$$

The van't Hoff equation was used to determine ΔH:

$$log\left(\frac{K_2}{K_1}\right) = \frac{-\Delta H}{2.303R}\left(\frac{T_2 - T_1}{T_1 T_2}\right)$$

Alternatively, ΔH was obtained from the slope of a plot of lnK versus 1/T, as described by:

$$logK = -\frac{\Delta H}{2.303R}\frac{1}{T} + constant$$

Finally, ΔS was calculated using:

$$\Delta G = \Delta H - T\Delta S$$

3.5. Nanoparticle Characterization

The quantity of unloaded insulin in the supernatant was calculated by UV-Vis spectrophotometer at 274 nm. All analyses were carried out in triplicate. The insulin loading and association efficiencies were measured:

$$Loading\ efficiency\ \% = \frac{Total\ amount\ of\ drug - Amount\ of\ unbound\ drug}{Nanoparticles\ weight}\ 100$$

$$Association\ efficiency\ \% = \frac{Total\ amount\ of\ drug - Amount\ of\ unbound\ drug}{Total\ amount\ of\ drug}\ 100$$

3.6. In Vitro Release Study

Simulated intestinal fluid (SIF, pH = 6.8) was selected as the release medium because insulin is unstable under gastric acidic conditions (pH ~ 2.0) and is primarily absorbed in the intestinal environment. The in vitro release profile of insulin was evaluated using the dialysis bag method. Insulin-loaded CS/HP-β-CD/sodium TPP NPs (equivalent to 1 mg/mL insulin) were placed inside a regenerated cellulose dialysis membrane (molecular weight cutoff appropriate for retaining insulin). The dialysis bag was immersed in 30 mL of SIF

(pH = 6.8) and maintained at 37°C under sink conditions. The receptor medium was continuously agitated at 330 rpm using a magnetic stirrer to ensure homogeneity and prevent concentration gradients. At predetermined time intervals, 2 mL aliquots were withdrawn and immediately replaced with an equal volume of fresh, pre-warmed SIF to maintain constant volume and sink conditions. The insulin concentration in each sample was determined spectrophotometrically at 274 nm against a calibration curve, and cumulative drug release was calculated (37).

The SIF was prepared according to standard protocols for intestinal drug release testing, consisting of 75 mM potassium dihydrogen phosphate (KH_2PO_4). The pH was adjusted to 6.8 ± 0.1 using 1 N NaOH, as insulin is unstable under gastric acidic conditions (pH ~ 2.0) and is primarily absorbed in the intestinal environment (pH ~ 6.8). The inclusion of sodium dodecyl sulfate (SDS) in SIF for insulin release studies is unusual and may denature the protein; therefore, SDS was omitted in the final protocol to preserve insulin integrity (38). All experiments were performed in triplicate (n = 3), and results are reported as mean ± standard deviation. Release efficiency (RE) was calculated as follows:

$$Release\ efficiency\ (RE) = (\ A_t / A_{encapsulated}\ ) \times 100$$

Where A_t is the absorbance of insulin at time t, and $A_{encapsulated}$ represents the absorbance corresponding to the total amount of encapsulated insulin.

4. Results

4.1. Optimization of Nanoparticle Size Against the Concentration of Its Components

The CS/HP-β-CD/sodium TPP NPs were prepared via ionotropic gelation (32), which relies on electrostatic interactions between the protonated amino groups of CS (positively charged at acidic pH) and TPP anions (negatively charged). The HP-β-CD is electrically neutral under these conditions and does not participate directly in ionic crosslinking; instead, it was incorporated to enhance insulin complexation and solubility. The effect of CS concentration on NP formation was evaluated in the presence of HP-β-CD. A CS concentration of 0.2% (w/v) yielded the smallest NPs (62.5 nm, Table 1, row 2). Notably, incorporation of HP-β-CD — at a fixed concentration of 6 mM across experiments (Table 1 rows 2 - 4) — did not significantly alter NP size. In contrast, TPP concentration profoundly influenced particle dimensions. Deviating from the optimal TPP concentration of 1.5 mg/mL — either by decreasing it to 1 mg/mL or increasing it to 2 mg/mL — resulted in larger NPs, with sizes increasing to 88.1 nm and 125 nm, respectively (Table 1 rows 5 and 6).

The results indicated that increasing the CS concentration led to a modest increase in NP yield. Among all tested formulations, the composition containing 0.2% (w/v) CS, 1.5 mg/mL sodium TPP, and 6 mM HP-β-CD was identified as optimal. This formulation produced the smallest NPs (62.5 nm) while maintaining a high production yield (38.1%) and favorable drug-loading properties. Consequently, it was selected for all subsequent characterization and in vitro drug release studies.

4.2. Characterization of the Optimized Prepared Nanoparticle

The optimized CS/HP-β-CD/sodium TPP NPs were characterized using a combination of analytical techniques, including UV-Vis and FT-IR spectroscopy, and SEM.

4.2.1. UV-Visible Analysis

All UV-Vis measurements were performed after appropriate dilution to ensure that absorbance values remained within the linear and reliable range of the spectrophotometer (A < 2.0). Although the spectra of different components partially overlap due to the common solvent system (acetate buffer, pH = 4.6), distinct shifts in λmax confirm the successful formation of intermediate complexes and final nanocomposites (Figures 1 and 2).

4.2.2. Fourier-Transform Infrared Analysis

The strong and broad absorption peak in the range of 3400 - 3500 cm^{-1} in all three spectra is attributed to the presence of hydroxyl groups (O–H stretching vibrations) in all three CS, HP-β-CD, and TPP compounds. The conjugation of the NH_2 functional group with the carbonyl group causes a reduction in C=O vibration to 1641 cm^{-1} for CS, which was observed at 1636 cm^{-1} and 1664 cm^{-1} for CS/TPP and CS/HP-β-CD/TPP, respectively. This shift shows the carbonyl's ability for intermolecular

Table 1. Effect of Different Concentrations of Chitosan, Tripolyphosphate, and 2-Hydroxypropyl-β-Cyclodextrin on the Size and Yield of Nanoparticles Produced by the Ionic Gelation Method (N = 3)

Rows	CS (%)	TPP (mg/mL)	HP-β-CD (mM)	Size (nm, mean ± SD)	Production Yield (% ± SD)
1	0.1	1.5	6	73.2 ± 1.8	39.1 ± 1.5
2	0.2	1.5	6	62.5 ± 1.2	38.1 ± 1.4
3	0.2	1.5	4	67.1 ± 1.6	29.2 ± 1.7
4	0.2	1.5	8	70.2 ± 1.4	39.2 ± 1.6
5	0.2	1	6	88.1 ± 2.1	40.1 ± 1.3
6	0.2	2	6	125.0 ± 3.5	35.7 ± 1.8
7	0.3	2	6	234.4 ± 5.3	39.4 ± 1.9
8	0.4	2	6	515.6 ± 7.3	43.6 ± 2.1

Abbreviations: CS, chitosan; TPP, tripolyphosphate; HP-β-CD, 2-hydroxypropyl-β-cyclodextrin.

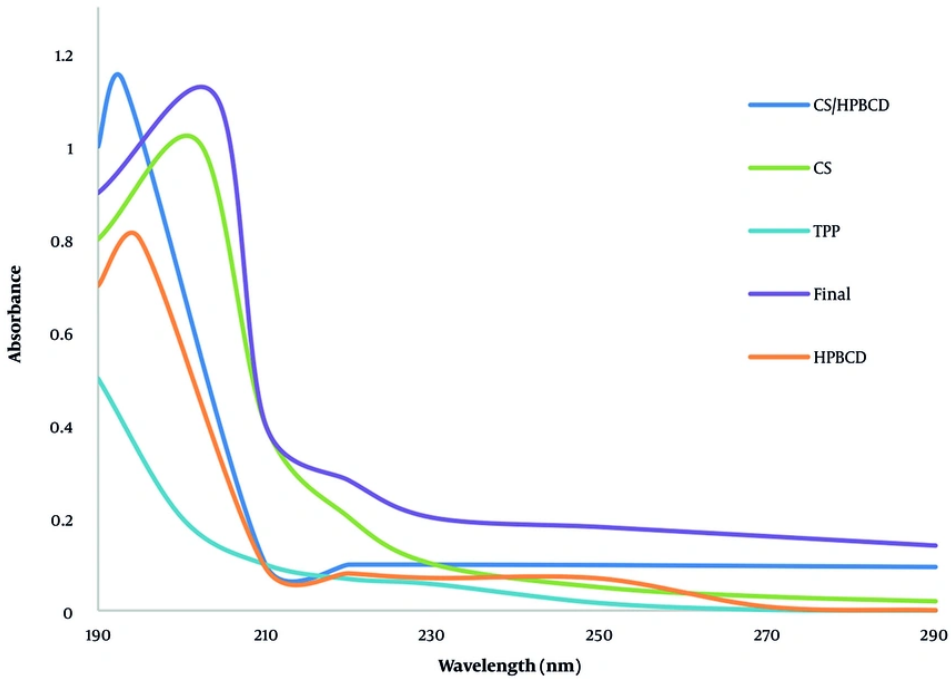

Figure 1. UV-Vis absorption spectra of chitosan (CS), 2-hydroxypropyl-β-cyclodextrin (HP-β-CD), sodium tripolyphosphate (TPP), and their optimized CS/HP-β-CD/TPP nanocomposite in acetate buffer (pH = 4.6) at 25°C

hydrogen bonding as a donor. The absorption at 1116 cm^{-1} in CS is related to the C–O–C ethereal group and can be observed with lower intensity for CS/TPP and CS/HP-β-CD/TPP, indicating oxygen's role as an intermolecular hydrogen bonding donor. The significant peak observed at 1215 cm^{-1} in CS/TPP is related to the P–O bond of TPP. This, however, is observed at a lower intensity in the CS/HP-β-CD/TPP wave due to shielding or encapsulation in the HP-β-CD cavity. Markedly, this peak is absent in the unmodified CS wave (Figure 3).

Now, after the absorption of insulin over the CS/HP-β-CD/TPP complex, its FT-IR spectrum was also recorded (Figure 4). This spectrum closely resembles that of its precursor, with two additional peaks at 1157 cm^{-1} and

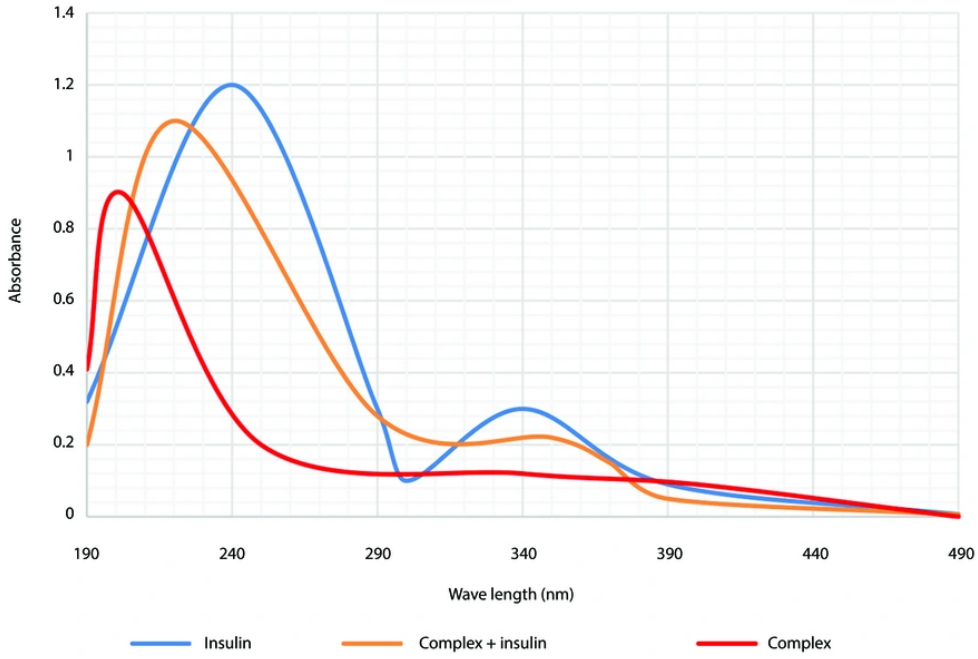

Figure 2. UV-Vis spectra of free insulin, blank chitosan (CS)/2-hydroxypropyl-β-cyclodextrin (HP-β-CD)/sodium tripolyphosphate (TPP) nanoparticles (NPs), and insulin-loaded CS/HP-β-CD/TPP nanocomposite, confirming successful encapsulation (pH = 4.6, 25°C).

1248 cm^{-1} present in the CS/HP-β-CD/TPP/insulin complex, which are associated with C–N and partially double C=N bonds due to resonance with the carbonyl group of insulin, a feature absent in the CS/HP-β-CD/TPP complex. These spectral shifts and newly emerged peaks collectively confirm successful ionic crosslinking, CD incorporation, and insulin loading within the CS/HP-β-CD/TPP nanocarrier.

4.2.3. Scanning Electron Microscopy Analysis

The morphology and surface texture of the synthesized CS/HP-β-CD/sodium TPP NPs were examined by SEM. As shown in Figure 5, the size and structural features of the NPs varied with changes in CS and TPP concentrations, while the HP-β-CD concentration was held constant at 6 mM.

The NPs exhibited a quasi-spherical morphology in both formulations. This shape is characteristic of CS-based NPs prepared via ionic gelation, which typically yield a porous, sponge-like internal structure. Consequently, minor morphological differences arising from the incorporation of β-CD are likely to be subtle and complex to discern by conventional SEM.

4.3. Characterization of Drug-Loaded Nanoparticles

Insulin was used as a model macromolecular drug, and insulin-loaded NPs were prepared by incorporating insulin into the CS/HP-β-CD/TPP nanocarrier during the NP formation process. The phase solubility profile of insulin in the presence of the nanocomposite is presented in Figure 6.

The plot shows a typical AL-type solubility curve classified by Higuchi and Connors at different temperatures, indicating that a soluble complex was formed (35). The solubility of insulin increased linearly as a function of nanocomposite concentration. As expected, insulin molecules exhibit a marked increase in their solubility with increasing nanocomposite concentration (Table 2).

Furthermore, stability constants (K_S) were estimated for the inclusion complex using thermodynamic parameters like ΔG, ΔH, and ΔS at different

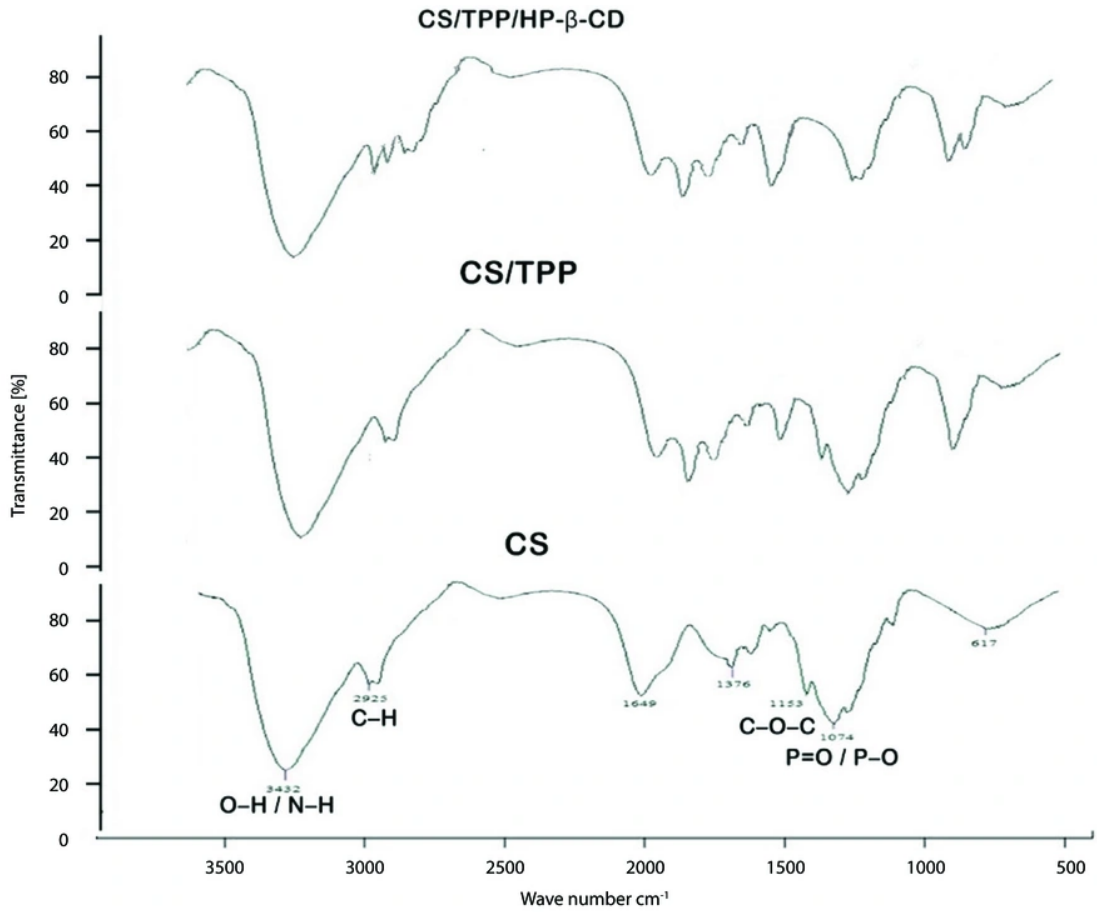

Figure 3. Fourier-transform infrared (FT-IR) spectra of chitosan (CS), CS/tripolyphosphate (TPP), and CS/TPP/2-hydroxypropyl-β-cyclodextrin (HP-β-CD) nanoparticles (NPs), showing characteristic functional group interactions

temperatures. Table 3 presents the corresponding 1:1 apparent stability constants. Notably, the stability constant decreased with increasing temperature, likely due to the weakening of non-covalent interactions — particularly van der Waals forces and hydrophobic interactions (39).

4.4. In Vitro Release Study

The in vitro release profile of insulin from the optimized NP formulation (0.2% CS, 1.5 mg/mL TPP, and 6 mM HP-β-CD), which exhibited the most favorable physicochemical characteristics (e.g., particle size, yield, and loading efficiency; Table 1), is shown in Figure 7. Release studies were conducted in SIF (pH = 6.8) at 37°C, with insulin release monitored in real time via UV-Vis spectrophotometry. As illustrated in Figure 7, approximately 70% of the encapsulated insulin was released within the first 20 minutes.

5. Discussion

Based on the data in Table 1, the formulation containing 0.2% (w/v) CS, 1.5 mg/mL TPP, and six mM HP-β-CD was selected as the optimized nanocarrier. This composition produced the smallest NPs (62.5 nm) with a high production yield (38.1%) and demonstrated superior performance in preliminary loading tests. All subsequent experiments — including drug loading, phase solubility, FT-IR, UV-Vis, and in vitro release — were conducted using this optimized formulation exclusively. The findings indicate that TPP operates synergistically

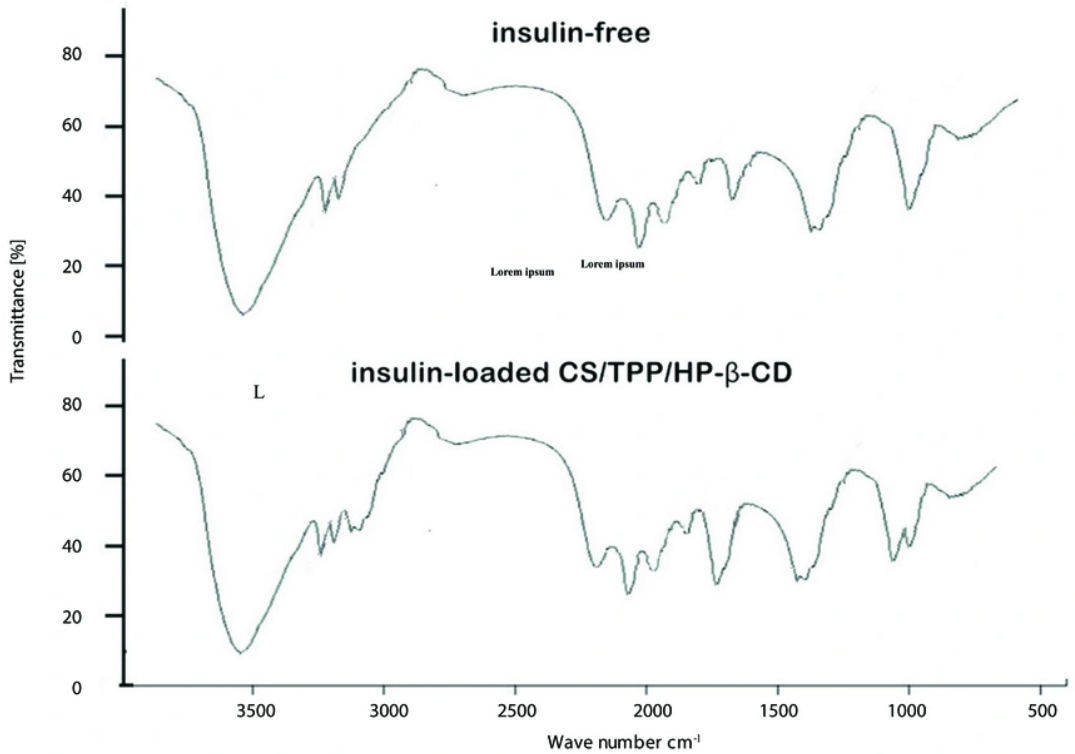

Figure 4. Fourier-transform infrared (FT-IR) spectra of insulin-free and insulin-loaded chitosan (CS)/tripolyphosphate (TPP)/2-hydroxypropyl-β-cyclodextrin (HP-β-CD) nanocomposite, highlighting C-N and C=N peaks (1157 and 1248 cm^{-1}) confirming insulin incorporation

with polyanionic CDs in the production of NPs. In summary, the neutral CD HP-β-CD, which demonstrates minimal affinity for CS, is integrated to a limited degree and has an insignificant impact on the NP assembly process. Anionic CD derivatives, which facilitate robust electrostatic crosslinking with CS, are effectively integrated and significantly improve NP yield. The noted decrease in particle size may be ascribed to enhanced ionic interactions between CS and the anionic CDs, which presumably facilitate the compaction of the polymeric network. Conversely, elevated concentrations of anionic CDs may promote the establishment of more nucleation sites upon interaction with CS, resulting in the production of a more substantial quantity of NPs with smaller dimensions.

Unlike differences in CS concentration, even slight alterations in TPP quantity markedly increased particle aggregation and clumping. This behavior can be explained by the significant disparity in molecular weights between CS and TPP. The CS's elevated molecular weight results in significant mass variations corresponding to minor alterations in molar quantity, thereby promoting the creation of well-dispersed NPs — especially when CS concentration is adequately diminished to restrict the availability of monomeric units. In contrast, TPP, due to its relatively low molecular weight, has a nearly proportionate connection between mass and molar concentration; therefore, minor changes in TPP mass result in a significant increase in the number of crosslinking molecules. The overabundance of TPP facilitates excessive ionic crosslinking with CS chains, leading to significant aggregation. At high concentrations, TPP promotes the development of hydrogen-bonded CS networks, facilitating the production of elongated nanofibrous structures instead of separate NPs. These data emphasize the necessity of utilizing a molar ratio,

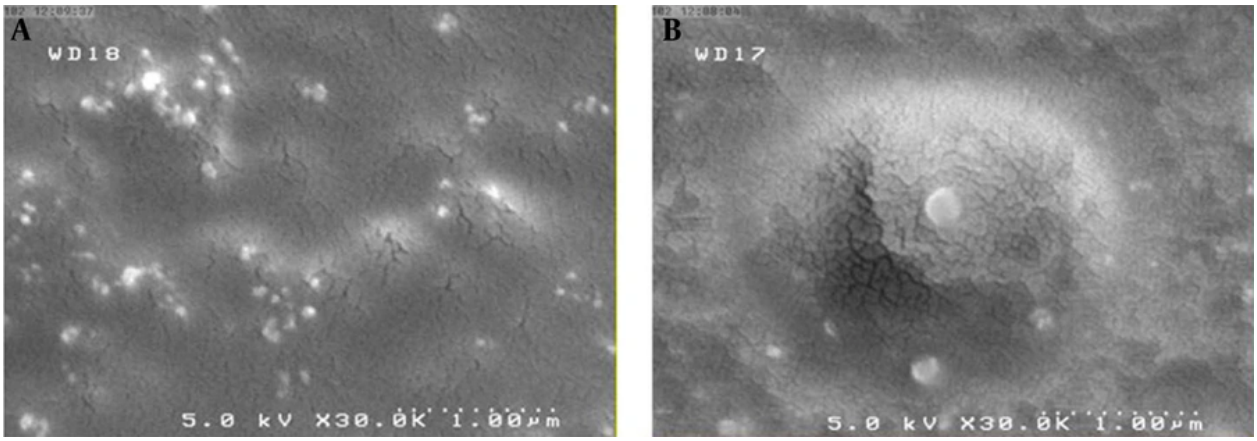

Figure 5. Scanning electron microscopy (SEM) micrographs of chitosan (CS)/2-hydroxypropyl-β-cyclodextrin (HP-β-CD)/tripolyphosphate (TPP) nanoparticles (NPs): (a) Optimized formulation (0.2% CS, 1.5 mg/mL TPP, six mM HP-β-CD) and (b) a non-optimized control formulation (0.3% CS, 2 mg/mL TPP, six mM HP-β-CD), illustrating the impact of polymer and crosslinker concentration on particle size and morphology

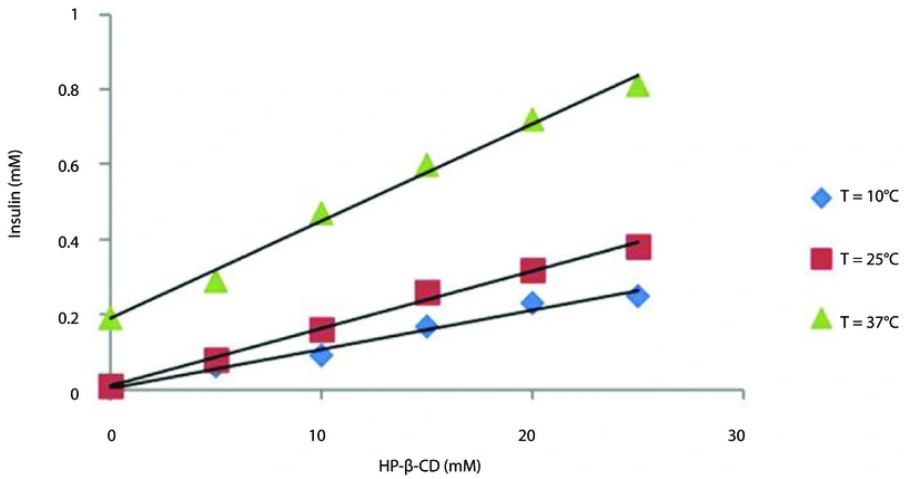

Figure 6. Phase solubility diagrams of insulin in the presence of increasing concentrations of chitosan (CS)/2-hydroxypropyl-β-cyclodextrin (HP-β-CD)/tripolyphosphate (TPP) nanocomposite at 10, 25, and 37°C (pH = 4.6), showing AL-type linear solubility enhancement (data are presented as mean ± SD, n = 3).

instead of a basic mass-based ratio, of CS to TPP for the attainment of controlled and reproducible NP synthesis.

Nonetheless, determining an exact molar ratio between CS and TPP is difficult due to the notably high and polydisperse molecular weight of CS. Formulation optimization can be effectively attained by consistently adjusting the concentrations of both components. In these investigations, precise modifications to TPP concentration are minimal, but CS concentration can be altered throughout a broader spectrum without affecting reproducibility. It has been shown that increased concentrations of β-CD facilitate particle aggregation and result in a larger hydrodynamic diameter. This effect is mainly ascribed to the self-assembly of CD-based complexes in aqueous

Table 2. Insulin Loading and Release Efficiency in Nanoparticles at Different Temperatures and Different Nanocarrier Concentrations (N = 3)

Rows	Temperature (°C)	NPs Concentration (mM)	Loading Efficiency (% ± SD)	Encapsulation Efficiency (% ± SD)
1	10	5	42.9 ± 2.1	94.5 ± 1.5
2	10	10	46.8 ± 1.7	92.6 ± 1.2
3	10	15	62.5 ± 1.9	86.2 ± 1.6
4	10	20	56.2 ± 2.3	81.3 ± 1.8
5	10	25	62.5 ± 2.0	79.5 ± 2.1
6	25	5	39 ± 2.5	93.5 ± 1.4
7	25	10	42.8 ± 1.6	86.9 ± 1.3
8	25	15	47.2 ± 2.2	78.7 ± 1.9
9	25	20	53.7 ± 1.8	73.9 ± 2.0
10	25	25	61.4 ± 2.4	68.9 ± 2.6
11	37	5	35.2 ± 2.7	76.3 ± 2.7
12	37	10	39.8 ± 2.0	61.8 ± 2.3
13	37	15	43.7 ± 2.5	5.09 ± 1.3
14	37	20	47.4 ± 1.6	41.1 ± 3.1
15	37	25	56.8 ± 1.9	33.8 ± 2.9

Abbreviation: NPs, nanoparticles.

Table 3. Thermodynamic Parameters of the Inclusion Process of Insulin in Nanoparticles

Rows	T(°C)	K1:1 (M-1)	ΔG (kJ/mol)	ΔH (kJ/mol)	ΔS (J/mol × K)
1	10	2638.56	-18535.82	-72105.66	-189.29
2	25	1291.686	-17748.59	-64206.38	-155.90
3	37	139.031	-12718.39	-53601.41	-131.88

environments, resulting in a significant increase in both mean particle size and Polydispersity Index (PDI).

The impact of CS concentration on NP size is significant: Elevated CS concentrations consistently produce larger NPs. Conversely, stable NP production was attainable within a limited TPP concentration range — specifically between 1.0 and 2.0 mg/mL. The mass ratio of CS to TPP significantly influences size distribution and colloidal stability.

Structurally, a single TPP molecule contains five negatively charged phosphate groups, allowing for the formation of up to five ionic crosslinks with protonated amino groups on CS chains. This stoichiometry indicates that roughly two CS glucosamine units can engage with one TPP molecule. A CS:TPP weight ratio of 5:1 (i.e., TPP at one-fifth the mass of CS) optimally enhances crosslinking efficiency, resulting in nearly total use of available amino groups and the creation of comparatively stable NPs. Concerning CD incorporation, low concentrations of β-CD may promote integration into the CS matrix, leading to larger assemblies. In contrast, at elevated concentrations, β-CD can promote a denser nanostructure via cumulative weak intermolecular interactions — such as hydrogen bonding and hydrophobic associations — between the CD cavities and the CS chain.

While direct assessment of insulin bioactivity (e.g., via cell-based assays or HPLC) was beyond the scope of this study, multiple lines of evidence support the preservation of insulin integrity: (1) The FT-IR spectra confirm the presence of intact amide bonds after encapsulation (Figure 4), (2) thermodynamic parameters indicate a stable, exothermic inclusion complex (Table 3), and (3) the AL-type phase solubility profile confirms molecular-level dispersion without aggregation (Figure 6). Future work will include direct bioactivity validation to quantify functional insulin recovery. This rapid release profile may be particularly advantageous for nasal delivery of insulin, where a burst release is often desirable to maximize absorption before mucociliary clearance eliminates the formulation from the nasal cavity. Given the limited fluid volume and short residence time in the nasal cavity, immediate

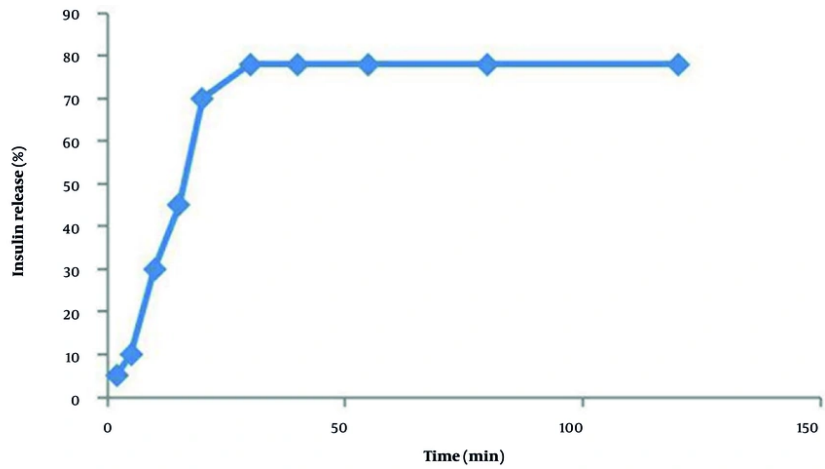

Figure 7. In vitro release profile of insulin from chitosan (CS)/2-hydroxypropyl-β-cyclodextrin (HP-β-CD)/tripolyphosphate (TPP) nanocarrier in simulated intestinal fluid (SIF, pH = 6.8) at 37°C under sink conditions (mean ± SD, n = 3), showing rapid release (~70% within 20 min, data are presented as mean ± SD; n = 3).

liberation of insulin upon contact with the nasal epithelium can enhance bioavailability (7, 10).

Although the nanocarrier exhibits rapid insulin release (~70% within 20 min), its value lies not in sustained release but in enabling non-invasive delivery through critical protective and functional roles. Free insulin in solution is rapidly degraded by proteolytic enzymes in the gastrointestinal (GI) tract or nasal cavity and exhibits poor mucosal permeability due to its large molecular size and hydrophilicity. In contrast, the TPP/HP-β-CD/CS nanocarrier: (1) Protects insulin from enzymatic degradation via encapsulation and complexation with HP-β-CD (as evidenced by negative ΔH and ΔS values indicating stable inclusion, Table 3); (2) enhances mucosal residence time through the mucoadhesive properties of CS; (3) promotes paracellular transport by transiently opening tight junctions between epithelial cells; and (4) stabilizes the protein structure during formulation and storage. These functions collectively increase the fraction of intact, bioactive insulin available for absorption — something a simple insulin solution cannot achieve.

5.1. Conclusions

In this paper, the ionic gelation technique is used to report the possibility of entrapping CDs within CS NPs. The results showed that the smallest NPs are formed with high binding capacity at the lowest polymer (CS) concentration. Other parameters like TPP concentration are also directly related to the NP size. An increase in the HP-β-CD concentration improves NP production efficiency. The introduced process upgrades hydrophobic drugs within the aqueous medium by developing a CD complex. Insulin is a macromolecular drug that can be combined with various nanocarriers, resulting in increased sensitivity to insulin. Such devices are of great interest as they can enhance the absorption of drugs with low solubility and low osmotic pressure and induce the protection of specific drug molecules by complexation and subsequent inclusion in the polymer matrix. Our results justify the engineered nanocarrier TPP/HP-β-CD/CS as a potential candidate for increasing the absorption of macromolecular drugs like insulin following oral or nasal administration accompanied by rapid drug release.

Acknowledgements

The authors would like to express their sincere gratitude to the laboratory staff and colleagues who provided technical assistance during the experimental work and manuscript preparation.

Footnotes

AI Use Disclosure: The authors declare that no generative AI tools were used in the creation of this article.

Authors' Contribution: Study concept and design: Amanollah Zarei-Ahmady; Acquisition of data: Ali Rajabiyan and Ghazaleh Shakiba-Maram; Analysis and interpretation of data: Amanollah Zarei-Ahmady and Mosadegh Keshavarz; Drafting of the manuscript: Ali Rajabiyan, Ghazaleh Shakiba-Maram, Amanollah Zarei-Ahmady, and Mosadegh Keshavarz; Critical revision of the manuscript for important intellectual content: Amanollah Zarei-Ahmady; Statistical analysis: Ali Rajabiyan and Mosadegh Keshavarz; Administrative, technical, and material support: Amanollah Zarei-Ahmady (Marine Pharmaceutical Science Research Centre, AJUMS); Study supervision: Amanollah Zarei-Ahmady.

Conflict of Interests Statement: The authors declare no conflict of interest.

Data Availability: The dataset presented in the study is available on request from the corresponding author during submission or after publication. The data are not publicly available due to the data containing sensitive health information that could compromise the privacy.

Ethical Approval: This study was approved by the Ethics Committee of Ahvaz Jundishapur University of Medical Sciences (IR.AJUMS.REC.1396.1012).

Funding/Support: This research was financially supported by the Vice-chancellor for Research Affairs of Ahvaz Jundishapur University of Medical Sciences, under grant number MPSRC-9601.

References

1. Ekore RI, Ekore JO, Ramadan H. Personalised Evidence, and Young Adults' Attitude and Behaviour towards Type 2 Diabetes Mellitus Preventive Lifestyle Measures. *Int J Diabetes Clin Res*. 2022;**8**:162.
2. Carino GP, Mathiowitz E. Oral Insulin Delivery. *Adv Drug Deliv Rev*. 1999;**35**(2-3):249-57. [PubMed ID: 10837700]. https://doi.org/10.1016/S0169-409X(98)00075-1.
3. De la Cruz-Concepción B, Flores-Cortez YA, Barragán-Bonilla MI, Mendoza-Bello JM, Espinoza-Rojo M. Insulin: A Connection Between Pancreatic B Cells and the Hypothalamus. *World J Diabetes*. 2023;**14**(2):76. [PubMed ID: 36926659]. [PubMed Central ID: PMC10011898]. https://doi.org/10.4239/wjd.v14.i2.76.
4. Khursheed R, Singh SK, Wadhwa S, Kapoor B, Gulati M, Kumar R, et al. Treatment strategies against diabetes: Success so far and challenges ahead. *Eur J Pharmacol*. 2019. [PubMed ID: 31449807]. https://doi.org/10.1016/j.ejphar.2019.172625.
5. Akbarian M, Farjadian F. Chitosan-Coated Glass Beads as Stabilizer of Insulin; a Novel Strategy for the Storage of Pharmaceutical Proteins. *ChemistrySelect*. 2024;**9**(40). e202402813. https://doi.org/10.1002/slct.202402813.
6. Shah P, Basant. *Strategies for Formulation and Systemic Delivery of Therapeutic Proteins*. Singapore: Springer Nature Singapore; 2023. p. 163-98. https://doi.org/10.1007/978-981-19-8249-1_6.
7. Illum L. Nasal delivery. The use of animal models to predict performance in man. *J Drug Target*. 1996;**3**(6):427-42. [PubMed ID: 8863136]. https://doi.org/10.3109/10611869609015963.
8. Tundisi LL, Ataide JA, Costa JS, De Freitas Coêlho D, Liszbinski RB, Lopes AM, et al. Nanotechnology as a tool to overcome macromolecules delivery issues. *Colloids Surf B Biointerfaces*. 2023. [PubMed ID: 36455361]. https://doi.org/10.1016/j.colsurfb.2022.113043.
9. Alberto M, Paiva-Santos AC, Veiga F, Pires PC. Lipid and polymeric nanoparticles: Successful strategies for nose-to-brain drug delivery in the treatment of depression and anxiety disorders. *Pharmaceutics*. 2022;**14**(2):2742. [PubMed ID: 36559236]. [PubMed Central ID: PMC9783528]. https://doi.org/10.3390/pharmaceutics14122742.
10. Kahraman E, Güngör S, Özsoy Y. *Nasal delivery of high molecular weight drugs: Recent trends and clinical evidence*. 2023. p. 253-77. https://doi.org/10.1007/978-3-031-23112-4_13.
11. Maram NS, Jelvehgari M, Vaccaro L, Lanari D, Mafakher L, Ahmady AZ. Preparation of vancomycin hydrochloride nanoparticles and survey of the factors influence their properties. *Orient J Chem*. 2017;**32**(2):575-83. https://doi.org/10.13005/ojc/330204.
12. Sarath Chandran C, Sajayan K, Kappally S, Gowtham M, Raj A, Swathy KK. *Chitosan-Based Drug Delivery Systems for Respiratory Diseases*. Singapore: Springer Nature Singapore; 2023. p. 201-15. https://doi.org/10.1007/978-981-19-7656-8_11.
13. Zhou Y, Li S, Tan W, Wei X, Chang Y, Yi Q, et al. Design, synthesis, and preparation of ultrasound-responsive curcumin-loaded chitosan nanocarriers. *Russ J Gen Chem*. 2023;**93**(1):108-15. https://doi.org/10.1134/S1070363223010152.
14. Rajabiyan A, Shakiba Maram N, Ghatrami ER, Zarei Ahmady A. Preparation of magnetic methotrexate nanocarrier coated with extracted hydroxyapatite of sea urchin (Echinometra mathaei). *Main Group Chem*. 2021;**20**(4):447-61. https://doi.org/10.3233/MGC-210043.
15. Jha R, Mayanovic RA. A review of the preparation, characterization, and applications of chitosan nanoparticles in nanomedicine. *Nanomaterials*. 2023;**13**(8):1302. [PubMed ID: 37110887]. [PubMed Central ID: PMC10140956]. https://doi.org/10.3390/nano13081302.
16. Kulkarni N, Jain P, Shindikar A, Suryawanshi P, Thorat N. Advances in the colon-targeted chitosan based multiunit drug delivery systems for the treatment of inflammatory bowel disease. *Carbohydr Polym*. 2022. [PubMed ID: 35450623]. https://doi.org/10.1016/j.carbpol.2022.119351.
17. Trapani A, Garcia-Fuentes M, Alonso MJ. Novel drug nanocarriers combining hydrophilic cyclodextrins and chitosan. *Nanotechnol*. 2008;**19**(8). [PubMed ID: 21825684]. https://doi.org/10.1088/0957-4484/19/18/185101.
18. Boczar D, Michalska K. Cyclodextrin inclusion complexes with antibiotics and antibacterial agents as drug-delivery systems—A pharmaceutical perspective. *Pharmaceutics*. 2022;**14**(7):1389. [PubMed ID: 35890285]. [PubMed Central ID: PMC9323747]. https://doi.org/10.3390/pharmaceutics14071389.

19. Ahamadi Azghandi MH, Keshavarz M, Zarei Ahmadi A, Parhami A, Iravani N. [Synthesis and characterization of MWCNT/PEG@ CD nanocomposite as carrier for sustained delivery of Acyclovir]. *Adv Mater New Coat*. 2017;**5**(20):1421-8. FA.
20. Kovacs T, Nagy P, Panyi G, Szente L, Varga Z, Zakany F. Cyclodextrins: Only pharmaceutical excipients or full-fledged drug candidates? *Pharmaceutics*. 2022;**14**(2):2559. [PubMed ID: 36559052]. [PubMed Central ID: PMC9788615]. https://doi.org/10.3390/pharmaceutics14122559.
21. Jansook P, Loftsson T. Self-assembled γ-cyclodextrin as nanocarriers for enhanced ocular drug bioavailability. *Int J Pharm*. 2022. [PubMed ID: 35278603]. https://doi.org/10.1016/j.ijpharm.2022.121654.
22. Matsubara K, Ando Y, Irie T, Uekama K. Protection afforded by maltosyl-β-cyclodextrin against α-chymotrypsin-catalyzed hydrolysis of a luteinizing hormone-releasing hormone agonist, buserelin acetate. *Pharm Res*. 1997;**14**(10):1401-5. [PubMed ID: 9358553]. https://doi.org/10.1023/A:1012120705408.
23. Lovatt M, Cooper A, Camilleri P. Energetics of cyclodextrin-induced dissociation of insulin. *Eur Biophys J*. 1996;**24**(5):354-7. [PubMed ID: 8766694]. https://doi.org/10.1007/BF00180377.
24. Zhang N, Li J, Jiang W, Ren C, Li J, Xin J, et al. Effective protection and controlled release of insulin by cationic β-cyclodextrin polymers from alginate/chitosan nanoparticles. *Int J Pharm*. 2010;**393**(1-2):213-9. [PubMed ID: 20394813]. https://doi.org/10.1016/j.ijpharm.2010.04.006.
25. Song M, Wang H, Chen K, Zhang S, Yu L, Elshazly EH, et al. Oral insulin delivery by carboxymethyl-β-cyclodextrin-grafted chitosan nanoparticles for improving diabetic treatment. *Artif Cells Nanomed Biotechnol*. 2018;**14**:774-82. [PubMed ID: 30280608]. https://doi.org/10.1080/21691401.2018.1511575.
26. Santana Gomes A, Silva Simplicio S, Marinheiro da Cunha Gonsalves JK. Chitosan Nanoparticles as a Potential Drug Delivery System in the Skin: A Systematic Review Based on In Vivo Studies. *ChemistrySelect*. 2024;**9**(43). e202402058. https://doi.org/10.1002/slct.202402058.
27. Suvarna V, Bore B, Bhawar C, Mallya R. Complexation of phytochemicals with cyclodextrins and their derivatives-an update. *Biomed Pharmacother*. 2022. [PubMed ID: 35339826]. https://doi.org/10.1016/j.biopha.2022.112862.
28. Ferreira L, Campos J, Veiga F, Cardoso C, Paiva-Santos AC. Cyclodextrin-based delivery systems in parenteral formulations: A critical update review. *Eur J Pharm Biopharm*. 2022;**178**:35-52. [PubMed ID: 35868490]. https://doi.org/10.1016/j.ejpb.2022.07.007.
29. Rezaei A, Vahidi SH, Nasrabadi M, Beyramabadi SA, Morsali A. Quantum chemical study of 2-hydroxypropyl-β-cyclodextrin and genipin-crosslinked chitosan nanocarriers functionalized with cytarabine anticancer drug. *J Mol Liq*. 2022. https://doi.org/10.1016/j.molliq.2022.120427.
30. Bensouiki S, Belaib F, Sindt M, Rup-Jacques S, Magri P, Ikhlef A, et al. Synthesis of cyclodextrins-metronidazole inclusion complexes and incorporation of metronidazole-2-hydroxypropyl-β-cyclodextrin inclusion complex in chitosan nanoparticles. *J Mol Struct*. 2022. https://doi.org/10.1016/j.molstruc.2021.131298.
31. Sajeesh S, Sharma CP. Cyclodextrin-insulin complex encapsulated polymethacrylic acid based nanoparticles for oral insulin delivery. *Int J Pharm*. 2006;**325**(1-2):147-54. [PubMed ID: 16859846]. https://doi.org/10.1016/j.ijpharm.2006.06.019.
32. Mi Y, Zhang J, Tan W, Miao Q, Li Q, Guo Z. Preparation of doxorubicin-loaded carboxymethyl-β-cyclodextrin/chitosan nanoparticles with antioxidant, antitumor activities and ph-sensitive release. *Mar Drugs*. 2022;**20**(5):278. [PubMed ID: 35621929]. [PubMed Central ID: PMC9146362]. https://doi.org/10.3390/md20050278.
33. Saokham P, Muankaew C, Jansook P, Loftsson T. Solubility of cyclodextrins and drug/cyclodextrin complexes. *Molecules*. 2018;**23**(5):1161. [PubMed ID: 29751694]. [PubMed Central ID: PMC6099580]. https://doi.org/10.3390/molecules23051161.
34. Calvo P, Remunan-Lopez C, Vila-Jato JL, Alonso MJ. Novel hydrophilic chitosan-polyethylene oxide nanoparticles as protein carriers. *J Appl Polym Sci*. 1997;**63**(1):125-32. https://doi.org/10.1002/(SICI)1097-4628(19970103)63:1<125::AID-APP13>3.0.CO;2-4.
35. Higuchi T, Connors KA. Phase-solubility Techniques. *Adv Anal Chem Instrum*. 1965;**4**:117-212.
36. Samuelsen L, Holm R, Schönbeck C. Simultaneous determination of cyclodextrin stability constants as a function of pH and temperature - a tool for drug formulation and process design. *J Drug Deliv Sci Technol*. 2021. https://doi.org/10.1016/j.jddst.2021.102675.
37. Patil P, Joshi P, Paradkar A. Effect of formulation variables on preparation and evaluation of gelled self-emulsifying drug delivery system (SEDDS) of ketoprofen. *Aaps Pharmscitech*. 2004;**5**(3):42. [PubMed ID: 15760075]. [PubMed Central ID: PMC2750265]. https://doi.org/10.1208/pt050342.
38. Zhang L, Jiang H, Zhu W, Wu L, Song L, Wu Q, et al. Improving the stability of insulin in solutions containing intestinal proteases in vitro. *Int J Mol Sci*. 2008;**9**(12):2376-87. [PubMed ID: 19330082]. [PubMed Central ID: PMC2635643]. https://doi.org/10.3390/ijms9122376.
39. Jain AC, Adeyeye MC. Hygroscopicity, phase solubility and dissolution of various substituted sulfobutylether β-cyclodextrins (SBE) and danazol-SBE inclusion complexes. *Int J Pharm*. 2001;**212**(2):177-86. [PubMed ID: 11165075]. https://doi.org/10.1016/S0378-5173(00)00607-4.